The effect of crystal anisotropy on the temperature-dependent mean square displacement, its temperature derivatives and second-order Doppler shift in zinc up to 600 K

1990 J. Phys.: Condens. Matter 2 7743

(http://iopscience.iop.org/0953-8984/2/38/003)

J. Phys.: Condens. Matter **2** (1990) 7743–7751. Printed in the UK

The effect of crystal anisotropy on the temperature-dependent mean square displacement, its temperature derivatives and second-order Doppler shift in zinc up to 600 K

S P Tewari† and Poonam Silotia
Department of Physics and Astrophysics, University of Delhi, Delhi-110007, India

Received 24 July 1989, in final form 23 April 1990

Abstract. Anisotropic mean square displacements, their temperature derivatives and second-order Doppler shift in the temperature range 0–600 K have been calculated in zinc by making use of the recently suggested anisotropic phonon frequency distribution function which takes into account the presence of planar modes. The calculated values of both the anisotropic mean square displacements and their temperature derivatives at various temperatures are in reasonable agreement with the corresponding experimental results. The effect of planar modes is found to be significant in the entire temperature range for all the three parameters studied.

1. Introduction

Zinc is a highly anisotropic crystal. It has a hexagonal close-packed structure with $c/a = 1.861$. Zinc therefore shows highly anisotropic behaviour in its various physical properties such as mean square displacement (MSD), mean square velocity, coefficient of thermal expansion and Grüneisen parameters. The values of these parameters along the c axis and perpendicular to it, i.e. in the basal plane are quite different. Further, recent measurements (Potzel *et al* 1983, 1984, Obenhuber *et al* 1987) of the Lamb–Mössbauer recoilless fraction (LMF) in ^{67}Zn at temperatures of 4.2, 20.8 and 47 K show that the ratio of LMF in the basal plane to that parallel to the c axis increases by as much as two orders when the temperature is raised from 4.2 to 47 K!

In a recent paper, we suggested an anisotropic frequency distribution function (FDF) of phonons (Tewari and Silotia 1989) which takes into account the presence of planar modes to explain successfully amongst other parameters the observed temperature variation in LMF along the c axis and perpendicular to it in the temperature range 4.2–47 K in zinc. In the present work, we utilise the same model of the phonon FDF to study for zinc

(i) the variation in the MSD up to 600 K,
(ii) the MSD derivatives in the temperature range 200–600 K and
(iii) the second-order Doppler shift in the temperature range 0–600 K.

† Author to whom all communications should be addressed.

0953-8984/90/387743 + 09 $03.50

At temperatures around 200 K, anharmonicity starts to play a role and this keeps on increasing with increase in temperature. We have taken the appropriate anharmonic effects into account in both the MSD and the MSD derivative studies. Comparison is made between the calculated and experimental results wherever available.

2. Mathematical formalism

2.1. Phonon frequency distribution function

The suggested phonon FDF (Tewari and Silotia 1989) for zinc in a given direction i, has the following form:

$$g(\nu_i) = \begin{cases} A_i \nu_i^2 & 0 \leqslant \nu \leqslant \nu_{0i} \\ B_i \nu_i & \nu_{0i} \leqslant \nu \leqslant \nu_{mi} \\ 0 & \nu > \nu_{mi} \end{cases} \tag{1}$$

where A_i and B_i are constants and can be determined using

(i) continuity of the two distribution functions at ν_{0i} and

(ii) the fact that the total number of modes along any direction is equal to N, where N is the total number of atoms in the crystal.

$g(\nu_i)$ along the c axis, i.e. $i = z$, and $g(\nu_i)$ perpendicular to the c axis, i.e. $i = x, y$, are different because the values of ν_{0i} and ν_{mi} are different.

The forms of FDF along the c axis and in the basal plane given by equation (1) are essentially due to the highly anisotropic crystal structure (Krumhansl and Brooks 1953, Firey *et al* 1983). Further, at low frequencies, only the ν^2 term contributes so that the specific heat variation at low temperatures is T^3 dependent, i.e. the contribution of two-dimensional modes is absent at low frequencies.

2.2. Mean square displacement

Using the dynamical model given by equation (1), one gets the following expression for the temperature-dependent displacement–displacement autocorrelation function in a given direction i:

$$\langle U_{T,i}^2(0,0)\rangle = \langle U_{T,i}^2(0,0)\rangle_{3D} + \langle U_{T,i}^2(0,0)\rangle_{2D} \tag{2}$$

where $\langle U_{T,i}^2(0,0)\rangle_{3D}$ and $\langle U_{T,i}^2(0,0)\rangle_{2D}$, respectively, are the contributions of three-dimensional and two-dimensional modes to $\langle U_{T,i}^2(0,0)\rangle$ and the expressions for these are as follows:

$$\langle U_{T,i}^2(0,0)\rangle_{3D} = \frac{\hbar^2}{Mk_B\Theta_{0i}}(\delta^2 - \tfrac{1}{3})^{-1}\left[\frac{1}{2} + \frac{2}{\varepsilon_3^2}\int_0^{\varepsilon_3}\frac{x}{\exp x - 1}\,dx\right] \tag{3}$$

$$\langle U_{T,i}^2(0,0)\rangle_{2D} = \frac{\hbar^2}{Mk_B\Theta_{0i}}(\delta^2 - \tfrac{1}{3})^{-1}\left[(\delta - 1) + \frac{2}{\varepsilon_3}\int_{\varepsilon_3}^{\varepsilon_2}\frac{1}{\exp x - 1}\,dx\right] \tag{4}$$

where M is the mass of the vibrating unit, k_B is the Boltzmann constant, $\delta = \nu_{mi}/\nu_{0i}$, $\Theta_{0i} = h\nu_{0i}/k_B$, $\Theta_{mi} = h\nu_{mi}/k_B$, $\varepsilon_3 = \Theta_{0i}/T$ and $\varepsilon_2 = \Theta_{mi}/T$.

At higher temperatures, where the anharmonic terms start to play their roles, we take the anharmonic MSD $\langle U^2_{T,i}(0,0)\rangle_{\text{anh}}$ in a given direction i (Crow *et al* 1989, Maradudin and Flinn 1963) to be of the following form:

$$\langle U^2_{T,i}(0,0)\rangle_{\text{anh}} = \langle U^2_{T,i}(0,0)\rangle[1 + T(2\alpha_i\gamma_i - 20k_B\gamma_{0i}/\alpha^2_{0i})] \tag{5}$$

where α_i and γ_i, respectively, are the coefficient of linear expansion and Grüneisen parameters in the direction i: $\alpha_{0i} = k_BT/\langle U^2_{T,i}(0,0)\rangle$ is the parameter which determines the strength of the harmonic potential; γ_{0i} is the quartic anharmonic parameter in the expansion of the potential energy of a crystal.

2.3. *Mean square displacement derivative*

The total MSD derivative $\langle U^2_{T,i}(0,0)\rangle'$ for a hexagonal crystal such as zinc in a given direction i consists of two terms (Skelton and Katz 1968, Nicklow and Young 1966):

(i) the derivative of $\langle U^2_{T,i}(0,0)\rangle$ w.r.t. temperature when c and a are constant and

(ii) the derivative due to change in c and a because of anisotropic expansion of the crystal.

These are given as follows:

$$\left[\frac{\partial\langle U^2_{T,i}(0,0)\rangle}{\partial T}\right]_{a,c} = \langle U^2_{T,i}(0,0)\rangle'_{a,c}$$

$$= \frac{\hbar^2}{3NMk_BT^2}\int_0^{\nu_{\max}} \frac{\exp(h\nu/k_BT)}{[\exp(h\nu/k_BT)-1)^2}\, g(\nu)\,\mathrm{d}\nu \tag{6}$$

$$\left[\left(\frac{\partial\langle U^2_{T,i}(0,0)\rangle}{\partial a}\right)_{c,T}\frac{\partial a}{\partial T} + \left(\frac{\partial\langle U^2_{T,i}(0,0)\rangle}{\partial c}\right)_{a,T}\frac{\partial c}{\partial T}\right]$$

$$= \frac{\hbar^2}{3NM}\alpha_i\gamma_i\left[\frac{1}{k_BT}\int_0^{\nu_{\max}} \frac{\exp(h\nu/k_BT)}{[\exp(h\nu/k_BT)-1]^2}\, g(\nu)\,\mathrm{d}\nu\right.$$

$$\left. + \int_0^{\nu_{\max}} \frac{1}{h\nu}\left(\frac{1}{\exp(h\nu/k_BT)-1} + \frac{1}{2}\right) g(\nu)\,\mathrm{d}\nu\right]. \tag{7}$$

Using equation (1), one gets the following expressions for (6) and (7), respectively:

$$\langle U^2_{T,i}(0,0)\rangle'_{a,c} = \frac{2\hbar^2}{Mk_B(3\Theta^2_{mi} - \Theta^2_{0i})}$$

$$\times\left[\frac{1}{\varepsilon_3}\int_0^{\varepsilon_3}\frac{x^2\exp x}{(\exp x-1)^2}\,\mathrm{d}x + \int_{\varepsilon_3}^{\varepsilon_2}\frac{x\exp x}{(\exp x-1)^2}\,\mathrm{d}x\right] \tag{8}$$

$$\left[\left(\frac{\partial\langle U^2_{T,i}(0,0)\rangle}{\partial a}\right)_{c,T}\frac{\partial a}{\partial T} + \left(\frac{\partial\langle U^2_{T,i}(0,0)\rangle}{\partial c}\right)_{a,T}\frac{\partial c}{\partial T}\right]$$

$$= \frac{2\hbar^2T\alpha_i\gamma_i}{Mk_B(3\Theta^2_{mi} - \Theta^2_{0i})}\left(\tfrac{1}{2}\varepsilon_3(\delta - \tfrac{1}{2}) + \frac{1}{\varepsilon_3}\int_0^{\varepsilon_3}\frac{x^2\exp x}{(\exp x-1)^2}\,\mathrm{d}x\right.$$

$$\left. + \int_{\varepsilon_3}^{\varepsilon_2}\frac{x\exp x}{(\exp x-1)^2}\,\mathrm{d}x + \frac{1}{\varepsilon_3}\int_0^{\varepsilon_3}\frac{x}{\exp x-1}\,\mathrm{d}x + \int_{\varepsilon_3}^{\varepsilon_2}\frac{1}{\exp x-1)}\,\mathrm{d}x\right). \tag{9}$$

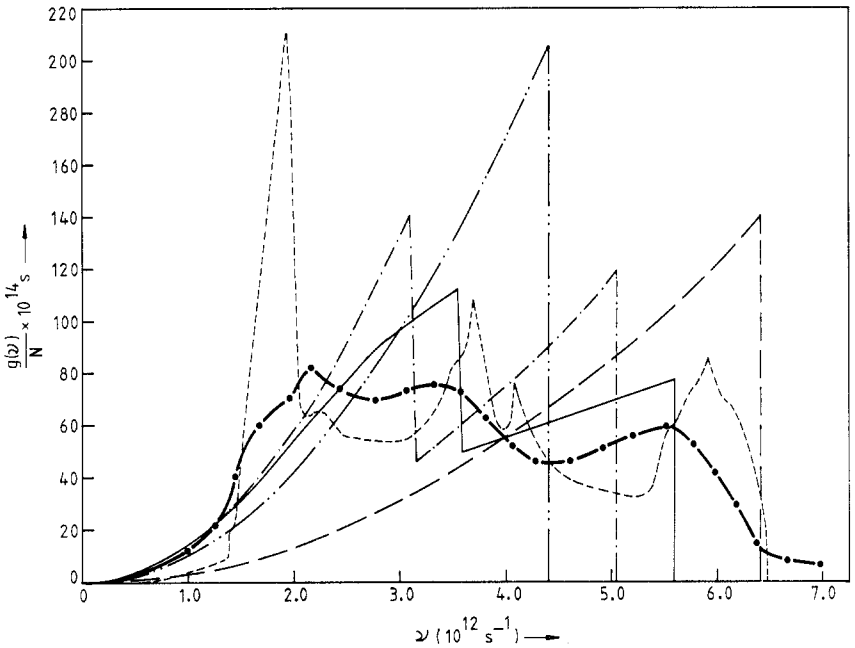

Figure 1. Comparison of the suggested phonon FDF for zinc with that given by other studies: ———, present model; —●—, experimental from neutron scattering (Eremeev *et al* 1976); — —, the Debye model, specific heat (Seidel and Keesom 1958); — · · —, the Debye model, LMF (Potzel *et al* 1984); — · —, the extended Debye model, LMF (Potzel *et al* 1984); – – – –, the modified axially symmetric model, lattice dynamics (Raubenheimer and Gilat 1967).

If we drop the planar mode contribution and suitably normalise the total number of modes, then equations (8) and (9) reduce to those given by Skelton and Katz (1968) which correspond to the isotropic phonon FDF.

2.4. Mean square velocity

For the evaluation of the temperature-dependent velocity–velocity autocorrelation function which is related to the second-order Doppler shift, we have used the same expression (7) as in our earlier paper (Tewari and Silotia 1989).

3. Results and discussion

As reported in our earlier paper (Tewari and Silotia 1989) the values of the set of characteristic parameters occurring in the FDF in equation (1) (Θ_{0z} = 100 K, Θ_{mz} = 170 K; Θ_{0xy} = 130 K, Θ_{mxy} = 269 K) explain successfully the temperature variation in the experimental MSD (Potzel *et al* 1983, 1984, Obenhuber *et al* 1987) in the temperature range 4.2–47 K along the *c* axis and in the basal plane for zinc. In figure 1, we have compared our total phonon FDF with that obtained in other studies (Potzel *et al* 1983, 1984, Raubenheimer and Gilat 1967) and that obtained experimentally by neutron scattering (Eremeev *et al* 1976). As is evident from the figure, the suggested phonon FDF

reproduces the gross structure of the experimental phonon FDF much better than the others do. Using the same values of the characteristic parameters and equations (2)–(4) we have calculated the MSD at higher temperatures up to 600 K both along the c axis and in the basal plane. The results of our calculations are plotted in figure 2 along with the experimental data obtained from x-ray diffraction (Skelton and Katz 1968). The calculated values shown by curve 3 are in rather good agreement with the corresponding experimental results for MSD in the basal plane in the entire temperature range. Along the c axis, the agreement between the calculated values given by curve 1 and the corresponding experimental results is quite good, about +4% up to 300 K. Even at higher temperatures the deviation from the observed MSD is not very large, being at the maximum about −20% at the highest temperature of 600 K. Thus the suggested anisotropic phonon FDF with the same set of values of the characteristic parameters is able to explain reasonably well the observed anisotropic MSD in the entire temperature range 0–600 K for zinc. We should point out that the total MSD given by our model is in good agreement with that given by Eremeev *et al* (1976) who have reported the total MSD in the temperature range 0–400 K obtained by using a FDF derived from the experimental results of neutron scattering. In figure 2 are also shown the contributions of three-dimensional modes to the MSD along the c axis and perpendicular to it by curves 2 and 4, respectively. Therefore, in both MSDs, i.e. $\langle U^2_{T,z}(0,0)\rangle$ and $\langle U^2_{T,xy}(0,0)\rangle$, the contribution of two-dimensional modes is very significant and keeps increasing with increase in temperature as is evident from figure 2.

For temperatures greater than 300 K, the experimental results in the MSD along the c axis have higher values than the corresponding calculated results using our model, curve 1. The difference between the two keeps on increasing with increase in temperature. However, since this difference is not very large along the c axis and is negligible in the basal plane even at 600 K, we have used equation (5) which, strictly speaking, is valid for a cubic lattice. Using the first two terms on the RHS of equation (5) along with $\gamma_z = 2.77$ (Barron and Munn 1967a) and the temperature-dependent α_z (Touloukian *et al* 1975), the values of $\langle U^2_{T,i}(0,0)\rangle_{\text{anh}}$ are evaluated. This results in an increase in the MSD at all the temperatures. We have then fixed the value of γ_{0z} by matching the calculated values of $\langle U^2_{T,z}(0,0)\rangle$ with the corresponding experimental result at 500 K. The value of γ_{0z} turns out to be about 2.6×10^{-14} erg Å^{-4}. Using this value of γ_{0z}, $\langle U^2_{T,z}(0,0)\rangle_{\text{anh}}$ is evaluated at other temperatures in the range 300–600 K and are shown in figure 2 by curve 5. These are in reasonable agreement with the corresponding experimental results and happen to lie within the errors of the results of Barron and Munn (1967b) which were obtained using thermodynamic data.

The effect of anharmonic terms has also been evaluated for $\langle U^2_{T,xy}(0,0)\rangle$ but it is so small that it cannot be distinctly shown in the figure.

As mentioned earlier, the total temperature MSD derivative $\langle U^2_T(0,0)\rangle'$ consists of two distinct physical terms given by equations (8) and (9) based on our dynamical model. Using equation (8), $\langle U^2_T(0,0)\rangle'_{a.c}$ $(=\langle U^2_{T,z}(0,0)\rangle'_{a.c} + 2\langle U^2_{T,xy}(0,0)\rangle'_{a.c})$ is evaluated at various temperatures in the range 200–600 K and its variation is shown by curve 1 in figure 3. Also plotted as full circles in the figure are the calculated results obtained from the values of characteristic Debye temperature $\Theta_{M'}(T)$, which reproduce $\langle U^2_T(0,0)\rangle'$ observed experimentally (Skelton and Katz 1968). The difference between these and those given by curve 1 is about +4% at 300 K and about −20% at 600 K. The temperature dependence given by the full circles is essentially due to the temperature dependence of $\Theta_{M'}(T)$. Such a temperature-dependent change in the phonon FDF has not been forced

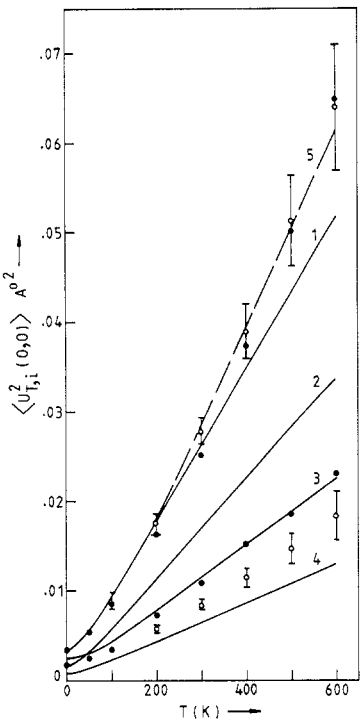

Figure 2. Comparison of the calculated values of MSD based on the suggested anisotropic dynamical model along the *c*-axis (curve 1) and in the basal plane (curve 3) at various temperatures for zinc in the range 0–600 K with the corresponding experimental results (●): ○, calculated results of Barron and Munn; curves 2 and 4, contributions of three-dimensional modes to curves 1 and 3, respectively; curve 5, total MSD along the *c* axis which includes the contribution of anharmonic terms also.

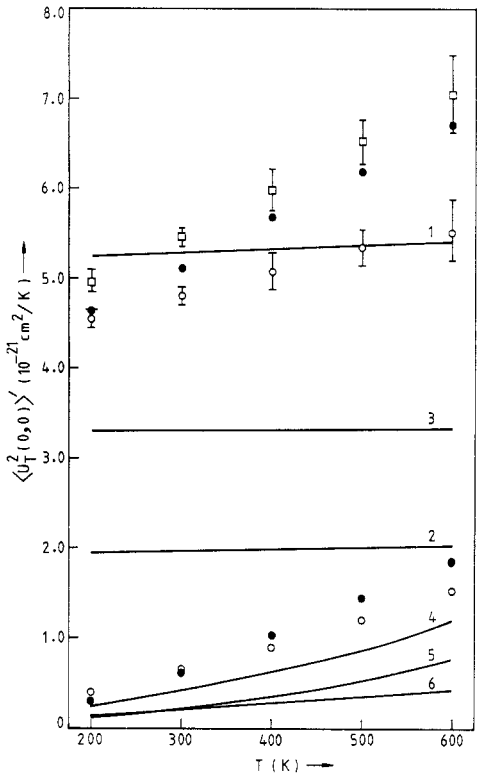

Figure 3. Comparison of the calculated values of the temperature derivative of MSD, using the suggested dynamical model for zinc at varying and constant *c* and *a* represented by curves 4 and 1, respectively, with the corresponding calculated results: ●, using $\Theta_{M'}(T)$ from the experimental results of the temperature derivative of total MSD; ○, results given by Barron and Munn; □, total derivative given by Barron and Munn; curves 2 and 3, contributions of two-dimensional and three-dimensional modes, respectively, to curve 1; curves 5 and 6 contributions of two-dimensional and three-dimensional modes, respectively, to curve 4.

in our calculations. The calculated values of $\langle U_T^2(0,0)\rangle'_{a,c}$ given by Barron and Munn (Skelton and Katz 1968) are represented by open circles along with their error bars. These lie closer to our calculated results, i.e. curve 1. Here too the temperature dependence is essentially because of the temperature-dependent $\Theta_M(T)$, the characteristic Debye temperature, which reproduces the total MSD results of Barron and Munn (1967b). In the figure are also shown the two-dimensional and three-dimensional contributions to $\langle U_T^2(0,0)\rangle'_{a,c}$ by curves 2 and 3, respectively. Here, too, we find that the contribution of two-dimensional modes is significant in the entire temperature range.

The calculated values of the MSD derivative given by equation (9) which takes into account the anisotropic expansion of the crystal, are shown in figure 3 by curve 4 along

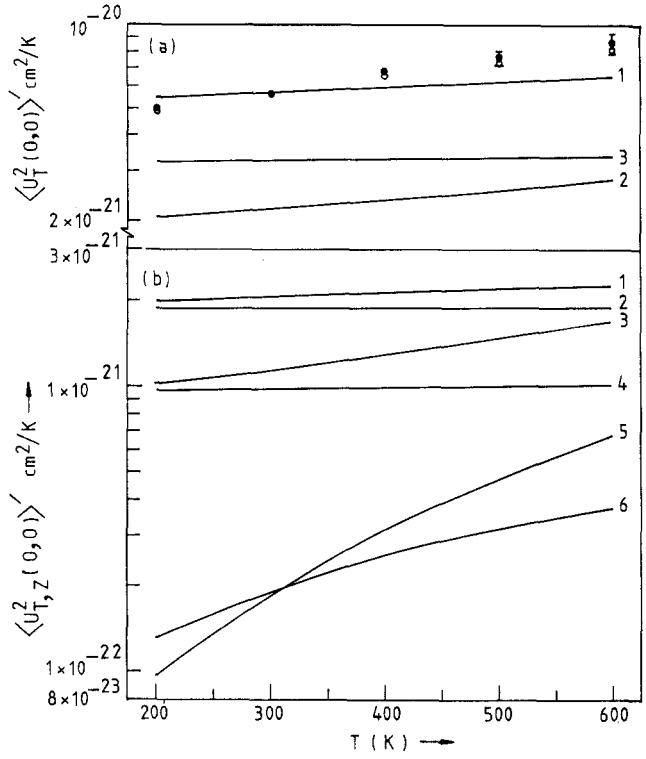

Figure 4. (*a*) Comparison of the calculated values of total MSD derivatives w.r.t. temperature (curve 1) for zinc with the corresponding experimental results (●): ○, calculated results of Barron and Munn corrected for constant volume anharmonic effects; curves 2 and 3, the contributions of two-dimensional and three-dimensional modes, respectively, to curve 1. (*b*) Details of the calculated values of temperature derivatives of the MSD for zinc along the *c* axis in the temperature range 200–600 K: curves 1 and 3, three-dimensional and two-dimensional contributions, respectively, to the total MSD derivative; curves 4 and 2, two-dimensional and three-dimensional contributions, respectively, to the temperature derivative of the MSD at constant volume; curves 5 and 6, two-dimensional and three-dimensional contributions, respectively, of the derivatives of MSD when *c* and *a* vary.

with the calculated values using $\Theta_{M'}(T)$. The difference between the two is about -32% at 300 K and about -36% at 600 K. Here, too, the calculated results of Barron and Munn (Skelton and Katz 1968) happen to lie close to our results. Also shown in the figure are the contributions of two-dimensional and three-dimensional modes given by curves 5 and 6, respectively. For temperatures greater than about 280 K, in contrast with $\langle U_T^2(0,0)\rangle'_{a,c}$, the two-dimensional contribution becomes greater than the corresponding three-dimensional contribution. In the figure, we have also shown the total $\langle U_T^2(0,0)\rangle'$ obtained from the data of Barron and Munn (Skelton and Katz 1968) denoted by open squares.

In figure 4(*a*), $\langle U_T^2(0,0)\rangle'$ is plotted with the experimental results denoted by full circles (Skelton and Katz 1968). The difference between the calculated and experimental results is about -0.6% at 300 K and about -24% at 600 K. The results of Barron and Munn corrected for the constant-volume anharmonic effect shown by open circles lie

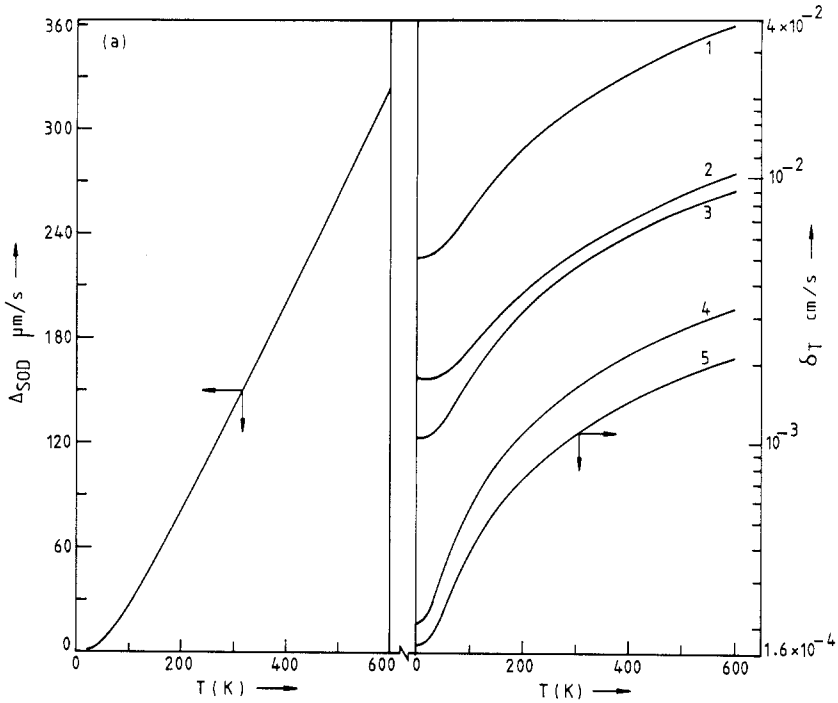

Figure 5. (*a*) Calculated second-order Doppler shift relative to that at 4.2 K in the temperature range 4.2–600 K for zinc. (*b*) Details of the calculated values of second-order Doppler shift in the temperature range 0–600 K for zinc based on the suggested anisotropic dynamical model; curve 1, the total second-order Doppler shift; curves 2 and 3, the two dimensional contributions to the second-order Doppler shift in the basal plane and along the *c* axis, respectively; curves 4 and 5, three-dimensional contributions to the second-order Doppler shift along the *c* axis and in the basal plane, respectively, for zinc.

close to our results in most of the temperature range. Two-dimensional and three-dimensional contributions to $\langle U_T^2(0,0)\rangle'$ are shown by curves 2 and 3, respectively. It is clear that, while the three-dimensional contributions remain more or less constant in the entire temperature range, the two-dimensional contribution varies and increases with increase in temperature.

In figure 4(*b*), we have plotted the details of our calculations of $\langle U_{T,z}^2(0,0)\rangle'$. Curves 2 and 4 represent the three-dimensional and two-dimensional contributions, respectively, to $\langle U_{T,z}^2(0,0)\rangle'$. Curves 5 and 6 represent the two-dimensional and three-dimensional contributions, respectively, to $\langle U_{T,z}^2(0,0)\rangle'$ when *c* and *a* vary. Curves 1 and 3 represent the total three-dimensional and two-dimensional mode contributions, respectively, to the total MSD along the *z* direction.

In figure 5(*a*) are plotted the results of our calculations of the second-order Doppler shift Δ_{SOD} at various temperatures relative to that at 4.2 K in the temperature range 4.2–600 K. Δ_{SOD} keeps increasing first non-linearly up to about 200 K, beyond which its variation is more or less linear up to 600 K. In figure 5(*b*) are plotted the three-dimensional and two-dimensional contributions of the second-order Doppler shift δ_T at various temperatures in the range 0–600 K. Both for the basal plane and along the *z* direction, the contribution of two-dimensional modes is much greater than the corresponding

contribution of three-dimensional modes at all temperatures. Curve 1 represents the total second order Doppler shift, and curves 2 and 3 represent the two-dimensional contribution to the second-order Doppler shift in the basal plane and along the c axis, respectively. Curves 4 and 5 denote the three-dimensional contributions to the second-order Doppler shift along the c axis and in the basal plane, respectively, for zinc.

4. Conclusion

From our study we conclude that the phonon FDF which takes into account explicitly the presence of planar modes is able to explain the observed temperature variation in the MSD in the temperature range 0–600 K with the same sets of characteristic parameters and yield values of the MSD derivatives and its components in reasonable agreement with the corresponding experimental results. In all the parameters studied, it is found that the contribution of two-dimensional modes is significant.

References

Barron T H K and Munn R W 1967a *Phil. Mag.* **15** 85–103
—— 1967b *Acta Crystallogr.* **22** 170–3
Crow M L, Schupp G, Yelon W B, Mullen J G and Djedid A 1989 *Phys. Rev.* B **39** 909–14
Eremeev I P, Sadikov I P and Chernyshov A A 1976 *Sov. Phys.–Solid State* **18** 960–4
Firey B, de Wette F W, de Rouffignac E and Alldredge G P 1983 *Phys. Rev.* B **28** 7210–8
Krumhansl J and Brooks H 1953 *J. Chem. Phys.* **21** 1663–9
Maradudin A A and Flinn P A 1963 *Phys. Rev.* **129** 2529–47
Nicklow R M and Young R A 1966 *Phys. Rev.* **152** 591–6
Obenhuber Th, Adlassnig W, Zankert J, Narger U, Potzel W and Kalvius G M 1987 *Hyperfine Interact.* **33** 69–88
Potzel W, Adlassnig W, Narger U, Obenhuber Th, Riski K and Kalvius G M 1984 *Phys. Rev.* B **30** 4980–8
Potzel W, Narger U, Obenhuber Th, Zankert J, Adlassnig W and Kalvius G M 1983 *Phys. Lett.* **98A** 295–8
Raubenheimer L J and Gilat G 1967 *Phys. Rev.* **157** 586–99
Seidel G and Keesom P H 1958 *Phys. Rev.* **112** 1083–8
Skelton E F and Katz J L 1968 *Phys. Rev.* **171** 801–8
Tewari S P and Silotia P 1989 *J. Phys.: Condens. Matter* **1** 5165–70, 7535–41
Touloukian Y S, Kirby R K, Taylor R E and Desai P D 1975 *Thermo-Physical Properties of Matter* (*TRPC Data Series 12*) (New York: Plenum)